HHS Public Access

Author manuscript

*Phys Med Biol*. Author manuscript; available in PMC 2019 January 09.

Published in final edited form as:

*Phys Med Biol*. ; 63(2): 025011. doi:10.1088/1361-6560/aa9a2f.

# The role of trapped bubbles in kidney stone detection with the color Doppler ultrasound twinkling artifact

**Julianna C. Simon**[1,2,*], **Oleg A. Sapozhnikov**[1,3], **Wayne Kreider**[1], **Michael Breshock**[1], **James C. Williams Jr**[4], and **Michael R. Bailey**[1,2]

[1]Center for Industrial and Medical Ultrasound, Applied Physics Laboratory, University of Washington, 1013 NE 40th St., Seattle, WA 98105, USA

[2]Department of Mechanical Engineering, University of Washington, Stevens Way, Box 352600, Seattle, WA 98195, USA

[3]Department of Acoustics, Physics Faculty, Moscow State University, Leninskie Gory, Moscow 119991, Russian Federation

[4]Department of Anatomy and Cell Biology, Indiana University School of Medicine, Indianapolis, IN, USA

## Abstract

The color Doppler ultrasound twinkling artifact, which highlights kidney stones with rapidly changing color, has the potential to improve stone detection; however, its inconsistent appearance has limited its clinical utility. Recently, it was proposed stable crevice bubbles on the kidney stone surface cause twinkling; however, the hypothesis is not fully accepted because the bubbles have not been directly observed. In this paper, the micron or submicron-sized bubbles predicted by the crevice bubble hypothesis are enlarged in kidney stones of five primary compositions by exposure to acoustic rarefaction pulses or hypobaric static pressures in order to simultaneously capture their appearance by high-speed photography and ultrasound imaging. On filming stones that twinkle, consecutive rarefaction pulses from a lithotripter caused some bubbles to reproducibly grow from specific locations on the stone surface, suggesting the presence of pre-existing crevice bubbles. Hyperbaric and hypobaric static pressures were found to modify the twinkling artifact; however, the simple expectation that hyperbaric exposures reduce and hypobaric pressures increase twinkling by shrinking and enlarging bubbles, respectively, largely held for rough-surfaced stones but was inadequate for smoother stones. Twinkling was found to increase or decrease in response to elevated static pressure on smooth stones, perhaps because of the compression of internal voids. These results support the crevice bubble hypothesis of twinkling and suggest the kidney stone crevices that give rise to the twinkling phenomenon may be internal as well as external.

### Keywords

twinkling artifact; Doppler ultrasound; kidney stone detection; cavitation; microbubbles

*Current Address for Julianna Simon: Graduate Program in Acoustics, The Pennsylvania State University, 201E Applied Science Building, University Park, PA, 16802 USA

## Introduction

Recent studies specifically investigating the color Doppler ultrasound “twinkling artifact” (which highlights stones with a mosaic of colors) on *in situ* human kidney stones identified by computed tomography (CT) found that 43–96% of stones twinkle (Aytaç and Özcan, 1999; Lee *et al.*, 2001; Gromov and Zykin, 2002; Turrin *et al.*, 2007; Park *et al.*, 2008; Dillman *et al.*, 2011; Winkel, Kalhauge and Fredfeldt, 2012; Kielar *et al.*, 2012; Sorensen *et al.*, 2013; Korkmaz *et al.*, 2014; Masch *et al.*, 2016). Several investigators have reported that surface roughness of a stone influences twinkling and surmise the rough interface produces random scattering of the ultrasound signal (Rahmouni *et al.*, 1996; Chelfouh *et al.*, 1998; Kamaya and Rubin, 2003; Alan *et al.*, 2011). Other investigators have found that twinkling depends on the stone composition, stone size, or the transmitted ultrasound frequency (Chelfouh *et al.*, 1998; Gao, Hentel and Rubin, 2012; Shivaprasad *et al.*, 2016; Shang *et al.*, 2017). Ultrasound machine settings - such as gain, transmitted power, pulse repetition frequency, and even “phase jitter” or internal noise - have also been suggested to explain twinkling (Aytaç and Özcan, 1999; Rubaltelli *et al.*, 2000; Kamaya and Rubin, 2003; Tanabe *et al.*, 2014). More recently, Lu et al. (2013) proposed that surface crevice bubbles cause twinkling because twinkling disappeared on *ex vivo* calcium oxalate monohydrate (COM) human kidney stones when exposed to hyperbaric pressures; twinkling resumed when the static pressure was reduced. Further, Lu et al. (2013) found that wetting the stone with ethanol, which has a lower surface tension than water, also eliminated twinkling on these COM stones presumably by reducing the presence of trapped surface bubbles. To extend these results, Li et al. (2014) investigated the use of twinkling to detect bubbles in bubble-based ultrasound treatments such as histotripsy and showed that twinkling was more sensitive than B-mode ultrasound or high-speed photography to the appearance of bubbles.

Kidney stones are very heterogeneous structures comprised of both inorganic crystals and an organic protein matrix (Williams *et al.*, 2010), yet it is unclear how stone composition, surface roughness, or even internal microarchitecture contributes to twinkling. The work by Lu et al. (2013) hypothesizing that surface crevice bubbles are the cause of the twinkling artifact focused solely on COM stones, the most common type of stone accounting for 55–76% of stones in North America (Worcester and Coe, 2008; Denstedt and Fuller, 2012). Researchers trying to categorize twinkling or even stone fragility in terms of stone composition or surface roughness have found variable and even contradictory results (Chelfouh *et al.*, 1998; Kamaya and Rubin, 2003; Williams *et al.*, 2003; Kim *et al.*, 2005; Shang *et al.*, 2017). Stones also contain varying degrees of voids, or volumes of low x-ray attenuation that can be identified by μCT; some are even visible with clinical CT (Zarse *et al.*, 2004; Williams *et al.*, 2010). While it is not clear what the voids contain, fluid or organic material are the leading hypotheses (Kim *et al.*, 2005), though there may also be gas pockets trapped within the voids (Fouke and Murphy, 2016). It therefore seems possible that the internal microarchitecture, surface roughness, and stone composition all contribute to kidney stone twinkling.

While it has been shown that bubbles display the twinkling artifact (Li *et al.*, 2014), there is still debate as to whether bubbles on kidney stones cause twinkling, in part, because the bubbles have not been directly observed (Tanabe *et al.*, 2014). The goal of this paper was to

enlarge the micron or submicron-sized surface crevice bubbles for visualization on five major kidney stone compositions, which would provide additional support for the crevice bubble hypothesis of twinkling. Surface crevice bubbles were modified by exposing the stones to: a lithotripter pulse with a transient negative-pressure tail which was expected to enlarge bubbles to a size sufficient for visualization with high-speed photography; static hyperbaric pressure, which was expected to shrink the bubbles and reduce twinkling; and static hypobaric pressure, which was expected to enlarge the bubbles and enhance twinkling.

## Methods

For all experiments, a research ultrasound system (Verasonics® V1, Kirkland, WA, USA) was used with a P4-2 transducer (2.5 MHz operating frequency, peak positive pressure $P_+ \approx$ 2 MPa, peak negative pressure $P_- \approx -1.5$ MPa (in water); Philips Ultrasound, Andover, MA, USA) and recorded twinkling at 12–15 fps (frames per second); an L7-4 transducer (5 MHz operating frequency; $P_+ \approx 2$ MPa, $P_- \approx -1$ MPa (in water)) was used for comparison in the hyperbaric study on COM stones. Nine to fourteen Doppler ensembles were repeated at 3000 Hz and consisted of 3 cycles each. Twinkling was quantified real-time in terms of twinkle power, or the magnitude of the color-Doppler ultrasound signal summed over a fixed, 20×20 pixel region of interest that included the kidney stone. The signals on the stone were at least two orders of magnitude larger than the Doppler signal off of the stone. Plots of twinkle power were then smoothed with 50-frame running average for analysis.

*Ex vivo* human kidney stones of 5–14 mm diameter were obtained and composition was determined through laboratory analysis (Zarse *et al.*, 2004; Williams *et al.*, 2010) with the numbers investigated shown in table 1. It is important to note that kidney stones are heterogeneous and composed of combinations of different crystals; classifications here indicate that each stone was >80% the primary composition listed. All stones were not exposed to every experimental condition. Artificial kidney stones, i.e., BegoStones and U30 stones, were also fabricated and used (Liu and Zhong, 2002; McAteer *et al.*, 2005). All stones were submerged in water for at least 48 hours prior to experimentation and all experiments were conducted in room temperature (~20°C) water, filtered to remove particulates larger than 5 μm and degassed with a Liqui-Cel Extra-Flow 2.5 × 8 gas contactor membrane with X50 fiber (Membrana, Charlotte, NC, USA) to 15–20% of oxygen saturation as measured with a dissolved oxygen meter (WTW Oxi 330i with a CellOx 325 probe, Weilheim, Germany).

### The Effect of Transient Negative Pressure

A lithotripter source that generates an intense acoustic pulse with a long negative-pressure tail was applied to transiently enlarge the surface crevice bubbles for visualization. A Dornier Compact S (Dornier MedTech, Munich, Germany) electromagnetic shock wave lithotripter was utilized to enlarge the bubbles so they could be visualized with high-speed photography (figure 1). The lithotripter was custom-modified to orient the lithotripter head horizontally for insertion into an acrylic water tank. Stones were placed in a custom, c-shaped holder that allowed for imaging with a high-speed camera (monochrome Fastcam APX-RS, Photron, San Diego, CA, USA) and a Philips/ATL P4-2 transducer without

material in the path of the lithotripter waves. A photogenic flash lamp (PowerLight 2500DR, Bartlett, IL, USA) front-lit the stone for high-speed photography at 10,000–150,000 fps. Stones were positioned pre-focal and off-axis within the lithotripter field, where the acoustic pressure within the pulse was predominantly negative. This allowed for control of bubble nucleation as the goal was to excite pre-existing bubbles on the surface of the stone while minimizing cavitation in the fluid around the stone; cavitation activity was monitored with a high-speed camera on the stone surface perpendicular to the propagation of the lithotripter wave. The measured waveform (FOPH 2000, RP Acoustics, Leutenbach, Germany) is shown in figure 1 (inset), with a peak positive pressure of 1.5 MPa, and peak negative pressure of 3 MPa.

### The Effect of Static Pressure

A custom-designed aluminum-walled hydraulic pressure chamber was used (figure 2) (Lu et al. 2013). A hydraulic hand pump was used to increase the pressure for hyperbaric exposures, whereas a vacuum pump and Erlenmeyer flask were used to reduce the pressure for the hypobaric exposures. Stones were imaged in the hydraulic pressure chamber through a 2.16-cm polystyrene window by an ultrasound imaging transducer and exposed to hyperbaric static pressures up to 9.7 MPa or hypobaric static pressures of 0.021 MPa. Reported pressures are absolute.

### The Contribution of Internal Microarchitecture to Twinkling

A subset of stones was imaged with micro computed tomography (μCT) before exposing the stones to hyperbaric static pressure. The stone specimens were scanned using a Skyscan 1172 μCT System (Bruker, Kartuizersweg, Belgium) at 60 kV, with final cubic voxel sizes ranging from 14–20 μm.

## RESULTS

### The Effect of Transient Negative Pressure

As bubbles on the kidney stone surface are presumably entrenched in crevices and thus invisible to direct observation, a pre-focal and off-axis lithotripter pulse was used to expand bubbles beyond individual crevices. Figure 3 shows the transient increase in twinkling and the creation or enlargement of bubbles on a COM stone in response to the lithotripter pulse (observed in 23/25 repetitions over 3 COM stones). Subsequent lithotripter pulses on the same COM stone shown in figure 3 (with minutes of delay between successive pulses) showed bubbles repeatedly grew from certain locations on the stone surface as shown in figure 4(a), suggesting the presence of pre-existing crevice bubbles. On this COM stone, 67–75% of visible bubbles (average of 24/35 bubbles, N=5) appeared from the same location in all five repetitions. When the temporal resolution of the high-speed camera was increased and the behavior of a single bubble cloud was visualized, the expansion, collapse, and rebound of this single bubble cloud was remarkably similar in all 4 repetitions as shown in figure 4(a, lower). Conversely, when a stone that did not twinkle with ultrasound alone (in this case an artificial BegoStone) was exposed to repeated lithotripter pulses, only 15–23% of bubbles arose in the same location with each pulse (average of 10/52 bubbles, N=4) and these were isolated to locations with visible imperfections on the stone surface (figure 4(b)).

Extending these observations to other stone compositions, a rough cystine stone that twinkled showed 46–60% of bubbles (average of 14/26 bubbles, N=4) emerged from same location. Other stones that did not twinkle or twinkled very weakly from ultrasound alone (twinkle power < $10^3$) such as smooth uric acid and brushite stones had few bubbles appear that did not overlap despite 20 (uric acid) or 39 (brushite) repetitions; tested U30 stones (which also did not twinkle with ultrasound alone) showed less than 13 out of more than 200 bubbles (hard to separate individual bubbles) had only partial overlap between repetitions (N=4). Figure 5 shows the generation of bubbles on the BegoStone surface also produced a strong twinkling signal for only one ultrasound imaging frame that coincided with the arrival of the lithotripter pulse (3 BegoStones, 15/17 repetitions); no surface erosion was observed. Categorizing stones by surface roughness extends these results. Rough stones such as the COM stone shown in figure 3 and all three of the tested cystine stones all had multiple crevices from which stable bubbles could repeatedly be expanded whereas smooth stones such as the BegoStone shown in figure 5 and the 3 tested uric acid and brushite stones required a lithotripter pulse to generate twinkling bubbles, which appeared with a variable distribution.

## The Effect of Elevated Static Pressure

Overall, the effect of elevated static pressure generally followed the trend observed by Lu et al. (2013) in that 69 of 90 experiments showed a reduction in twinkling from exposure to the elevated static pressure. The exact hyperbaric pressures required to suppress bubbles varied in replicated experiments even with the same stone, perhaps because of variations in the initial size or number of bubbles on the stone surface. Figure 6 shows plots of twinkle power taken 24 hours apart where the COM stone required half the pressure in (a) to reduce twinkling compared to (b) (0.41 MPa versus 0.79 MPa, respectively). Among the 8 tested COM stones and more than 42 experiments, the lowest pressure to diminish twinkling was 0.41 MPa; 3 of the COM stones showed little to no reduction in twinkling at the maximum pressure of 9.7 MPa. The 4 cystine stones used in the hyperbaric experiments performed similarly to COM stones, with hyperbaric thresholds to diminish twinkling between 0.41 MPa and 1.13 MPa. Conversely, twinkling was difficult to find on the 3 brushite and 6 uric acid stones (found only 17 times despite >50 trials) and was very weak when present, at least in this experimental scenario. This might be expected for these stone types as both uric acid and brushite stones have a measurable solubility in water and microscopic dissolution of the stone surface in water could release crevice bubbles. In 21 of 90 experiments, twinkling was found to increase rather than decrease with the elevated pressure, which was observed at times with replicated experiments in the same stone. Figure 7 shows examples of twinkling (a) increasing and (b) decreasing in the same brushite stone.

## The Effect of Reduced Static Pressure

In 3 COM stones, twinkling consistently increased as expected with hypobaric pressure as shown in figure 8(a). All other types of tested stones including cystine, uric acid, and brushite (figure 8(b)) consistently showed a decrease in twinkling when exposed to hypobaric pressures.

While these data are presented in terms of stone composition, observations suggest the response of twinkling to changes in static pressure may have been correlated with macroscopic surface roughness (as identified through visual analysis) over stone composition. Tested brushite and uric acid stones had smooth surfaces, whereas most of the tested COM and cystine stones were rough. A few smooth COM stones (n=3) were included and, in general, twinkling on these stones required more pressure for a response (if any) to be observed. However, the hypobaric exposure for a rough cystine stone did not cause twinkling to increase. Therefore, while surface roughness appears to contribute to the twinkling response for changesin pressure, surface roughness alone is insufficient to explain all of the nuances observed in these pressure studies.

### The Contribution of Internal Microarchitecture to Twinkling

Seven stones with low x-ray attenuation void fractions for the center slice from 2.3% to 23% were imaged with μCT before repeated hyperbaric exposures. Figure 9(a) shows the increase in twinkling for a COD stone exposed to hyperbaric pressures with the accompanying μCT image showing some areas of low x-ray attenuation surrounded by a relatively dense outer shell. Conversely, figure 9(b) shows a decrease in twinkling for a cystine stone exposed to hyperbaric pressures and the μCT image shows a scattering of low x-ray attenuation areas throughout the stone with no apparent outer shell. These low x-ray attenuation areas are likely indicative of fluid or the organic protein matrix (Kim *et al.*, 2005) and possibly contains pockets of trapped gas (Fouke and Murphy, 2016). Only two of the stones collected showed an immediate decrease in twinkling in response to an increase in pressure; these stones had the lowest void fractions of 2.3% and 3.7% with no outer shell. The other five stones had a dense outer shell and twinkling increased (at least initially) before decreasing. Compressing a stone with trapped gas or soft inclusions with a dense outer shell could give rise to structural changes that influence twinkling and there may be a relationship between the calculated void fraction of the center slice and the effect of static hyperbaric pressure on twinkling.

## Discussion

When the 7 stones that twinkled were exposed to a lithotripter pulse, microbubbles hypothesized to be stable but invisible in the surface crevices became visible and over half of these bubbles repeatedly arose from the same locations on the stone. Conversely, when repeated lithotripter pulses reached the 9 stones that did not twinkle and were smooth and flat, the bubble distribution was variable with few bubbles arising from the same location with each pulse. These bubbles likely arose from stochastic cavitation events as opposed to excitation of specific, robust bubble nuclei. Twinkling was also found to be modified by hyperbaric and hypobaric static pressures, suggesting that bubbles are the source of twinkling. However, the response of twinkling to changes in static pressures did not always follow such a simple explanation. It is possible that the initial bubble sizes affect the response to changes in static pressure; that is, bubbles that begin larger or smaller than resonance size may express opposite effects on twinkling. Two transducers with different central frequencies of 2.5 MHz and 5 MHz were used for the hyperbaric experiments on 3 COM stones and similar twinkle powers and hyperbaric thresholds upwards of 0.4 MPa to

reduce twinkling were observed for both transducers. Further, bubbles might not exist exclusively on the stone surface. Surface topography and the internal microarchitecture differed among all tested stones and may have influenced the response of the stones to variations in the static pressure.

On a macroscopic or direct visual level, kidney stones either have a rough surface, in which there are crevices for stable bubbles to reside, or a smooth surface where if stable bubbles exist they are either in microscopic crevices or near surface hydrophobic proteins. The results from the static pressure experiments and the lithotripter experiment suggest that stable bubbles are present in the crevices of rough-surfaced stones, but are not present (at least in sufficient quantities) on the surface of smooth stones. When stable bubbles are present, the size distribution would be expected to be variable and range from nanometers to 10's of microns in diameter based on scanning electron microscopy images of kidney stone surfaces (Grases et al., 1998). The Minnaert resonant air bubble radius of a free bubble in water for the 2.5 MHz source is approximately 1.8 μm, and bubbles near this size will scatter the ultrasound imaging pulse most efficiently (Leighton, 1994). The Minneart resonant frequency prediction does not include the effects of surface tension, which, along with the shape of the crevice stabilizes the bubble against dissolution and can be expected to influence the resonant bubble diameter (Apfel 1970, Crum 1979). Estimations of the Blake threshold at atmospheric pressures indicate that transient cavitation could be generated by the 0.5 MPa pressure amplitude diagnostic pulse (attenuated through the acrylic lens) for bubbles with radii larger than 0.14 μm. When the ambient pressure is increased to 0.4 MPa (absolute), the lowest pressure to eliminate twinkling in the rough-surfaced COM and cystine stones, initial bubble radii must exceed 0.5 μm for transient cavitation to occur, which is approaching the new radii for bubbles that were resonant at atmospheric pressures. While evidence suggests the presence of crevice bubbles, at least on rough stones, more information is needed about the bubble distribution on the kidney stone surface to fully understand the contribution of surface bubbles to twinkling.

Low x-ray attenuation volumes present on μCT images of kidney stones are indicative of the organic protein matrix, which may contain trapped gas and contribute to twinkling. The possibility that internal crevices may twinkle is supported by a BegoStone created in the lab that was found to twinkle when an air bubble became trapped during manufacturing (5/6 tested Bego/U30 stones do not twinkle). Stones with low x-ray attenuation volumes distributed throughout the stone without a dense outer shell (such as the cystine stone shown in figure 9(b)) showed an immediate decrease in twinkling when hyperbaric pressures were applied. The presence of internal gas pockets or soft inclusions contained within the dense outer shell of the stone could also explain why twinkling increased with pressure in some stones, i.e., compressing a stone with trapped gas or other soft inclusions could result in the enhancement of the stone shell deformation under excess static pressure, which in turn could give rise to structural changes including the appearance of microcracks on the stone surface that would harbor microbubbles. Stone composition could affect these microbubbles depending on the chemistry of the gas production. Nevertheless, as protein coverings on calcium oxalate crystals are much less than 1 micrometer wide (Khan, Finlayson and Hackett, 1984), high resolution scanning or transmission electron microscopy may be needed to detect any structural changes from hyperbaric exposures.

While care was taken to keep experimental conditions consistent, the variations in the results suggest that there are parameters of interest that were unaccounted for or that may be beyond our control. For example, repeated hyperbaric and hypobaric exposures likely change the bubble distribution and may cause temporary or permanent structural changes in the stone which could influence the results for repeated exposures on the same stone. Not all stones were used for every experiment and order of experiments were varied among stones. While no trends were observed based on experimental order or trends, the possibility of these temporary or permanent structural changes exist and are a source of future investigations. In addition, the μCT scans suggest that internal structure is extremely variable, even between stones identified as having similar compositions, which makes comparisons between stones difficult. During the analysis, surface roughness was identified as one of the parameters that may influence twinkling; however, this was found to be very difficult to quantify without access to specialized equipment. Due to the many structural factors found to influence twinkling, repeated experimentation on a relatively small subset of stones was used for this study to allow for thorough analysis of the factors that may influence twinkling.

## Conclusions

The results from these studies support the crevice bubble hypothesis of twinkling and suggest that kidney stone crevices may be internal as well as external. When stones that twinkle were exposed to a lithotripter pulse with a long negative tail, bubbles stabilized within the surface crevices became visible and repeatedly arose from the same locations or twinkling sites on the stone. Twinkling was found to be modified by hyperbaric and hypobaric static pressures, but not always following the simple expectation the increasing the pressure shrinks the bubbles and reduces twinkling. Surface topography and internal microarchitecture which can differ even in stones of the same composition were identified as two factors that influence twinkling. Hopefully, better understanding the role of surface crevice bubbles and the internal microarchitecture in twinkling will help researchers make twinkling appear more consistently on kidney stones so that it can transition into clinic as a valuable diagnostic tool.

## Acknowledgments

The authors would like to thank our collaborators at the Center for Industrial and Medical Ultrasound and at Indiana University School of Medicine. In particular, we would like to thank Brian MacConaghy for designing and building the pressure chamber as well as designing the stone holder for the lithotripsy experiments and Bryan Cunitz for his help with programming the ultrasound machine. We would also like to thank our funding sources including the National Space Biomedical Research Institute thought NASA NCC 9–58, the National Institute of Health NIDDK grant DK043881, and the Russian Foundation for Basic Research grant 17-02-00261.

## References

Alan C, Koçoğlu H, Kosar S, Karatag O, Ersay AR, Erhan A. Role of twinkling artifact in characterization of urinary calculi. Actas Urológicas Españolas (English Edition). 2011; 35(7):396–402. DOI: 10.1016/j.acuroe.2011.02.006

Apfel RE. Role of impurities in cavitation-threshold determination. J Acoust Soc Am. 1970; 48(5): 1179–1186.

Aytaç SK, Özcan H. Effect of color Doppler system on the twinkling sign associated with urinary tract calculi. J Clinical Ultrasound. 1999; 27(8):433–439. DOI: 10.1002/(SICI)1097-0096(199910)27:8<433::AID-JCU4>3.0.CO;2-1 [PubMed: 10477885]

Chelfouh N, Grenier N, Higueret D, Trillaud H, Levantal O, Pariente J-L, Ballanger P. Characterization of Urinary Calculi: In Vitro Study of "Twinkling Artifact" Revealed byColor-Flow Sonography. AJR. 1998; 171:1055–1060. [PubMed: 9762996]

Crum LA. Tensile strength of water. Nature. 1979; 278:148–149.

Denstedt, J., Fuller, A. Epidemiology of Stone Disease in North America. In: Talati, J.Tiselius, H-G.Albala, D., Ye, Z., editors. Urolithiasis: Basic Science and Clinical Practice. Springer-Verlag; London: 2012. p. 13-20.

Dillman JR, Kappil M, Weadock WJ, Rubin JM, Platt JF, DiPietro Ma, Bude RO. Sonographic twinkling artifact for renal calculus detection: correlation with CT. Radiology. 2011; 259(3):911–916. DOI: 10.1148/radiol.11102128 [PubMed: 21460031]

Fouke, B., Murphy, T. The Art of Yellowstone Science: Mammoth Hot Springs as a Window on the Universe. Crystal Creek Press; 2016.

Gao J, Hentel K, Rubin JM. Correlation Between Twinkling Artifact and ColorDoppler Carrier Frequency: Preliminary Observations in Renal Calculi. Ultrasound in Medicine and Biology. 2012; 38(9):1534–1539. DOI: 10.1016/j.ultrasmedbio.2012.04.011 [PubMed: 22698502]

Grases F, Costa-Bauza A, Garcia-Ferragut L. Biopathological crystallization: a general view about the mechanisms of renal stone formation. Adv Colloid Interface Sci. 1998; 74:169–194. [PubMed: 9561720]

Gromov A, Zykin B. Tissue Doppler imaging: Color Doppler for registration of ultrasouond-induced resonance of micro-concretions. Echography. 2002; 3:348–353. (in Russian).

Kamaya A, Rubin JM. Dependence on Machine Parameters Executive CouncilAward and Underlying Cause. AJR. 2003; 180:215–222. [PubMed: 12490508]

Khan SR, Finlayson B, Hackett R. Renal papillary changes in patient with calcium oxalate lithiasis. Urology. 1984; 23(2):194–199. [PubMed: 6695491]

Kielar AZ, Shabana W, Vakili M, Rubin J. Prospective evaluation of Doppler sonography to detect the twinkling artifact versus unenhanced computed tomography for identifying urinary tract calculi. J Ultrasound Med. 2012; 31(10):1619–25. Available at: http://www.ncbi.nlm.nih.gov/pubmed/23011625. [PubMed: 23011625]

Kim S, Hatt E, Lingeman J, Nadler R, McAteer J, Williams J. Cystine: Helical Computerized Tomography Characterization of Rough and Smooth Calculi in Vitro. J Urol. 2005; 174(4):1468–1471. DOI: 10.1097/01.ju.0000173636.19741.24 [PubMed: 16145473]

Korkmaz M, Aras B, Şanal B, Yücel M, Güneyli S, Koçak A, Uruç F. Investigating the clinical significance of twinkling artifacts in patients with urolithiasis smaller than 5 mm. Jap J Radiology. 2014; 32(8):482–486. DOI: 10.1007/s11604-014-0337-6

Lee J, Kim S, Cho J, Han D. Color and power doppler twinkling artifacts from urinary stones: Clinical observations and phantom studies. AJR. 2001; 176(6):1441–1445. DOI: 10.2214/ajr.176.6.1761441 [PubMed: 11373210]

Leighton, TG. The Acoustic Bubble. Academic Press Inc; San Diego: The Freely-Oscillating Bubble; p. 136-139.

Li T, Khokhlova T, Sapozhnikov O, O'Donnell M, Hwang J. A New ActiveCavitation Mapping Technique for Pulsed HIFU Applications - Bubble Doppler. IEEE Trans Ultrason Ferroelectr Freq Control. 2014; 61(10):1698–1708. DOI: 10.1037/emo0000122.Do [PubMed: 25265178]

Liu Y, Zhong P. BegoStone--a new stone phantom for shock wave lithotripsy research. J Acoust Soc Am. 2002; 112(4):1265–1268. DOI: 10.1121/1.1501905 [PubMed: 12398432]

Lu W, Sapozhnikov OA, Bailey MR, Kaczkowski PJ, Crum LA. Evidencefor Trapped Surface Bubbles as the Cause for the Twinkling Artifact in Ultrasound Imaging. Ultrasound Med Biol. 2013; 39(6):1026–1038. DOI: 10.1016/j.ultrasmedbio.2013.01.011 [PubMed: 23562014]

Masch WR, Cohan RH, Ellis JH, Dillman JR, Rubin JM, Davenport MS. Clinical effectiveness of prospectively reported sonographic twinkling artifact for the diagnosis of renal calculus in patients without known urolithiasis. American Journal of Roentgenology. 2016; 206(2):326–331. DOI: 10.2214/AJR.15.14998 [PubMed: 26797359]

McAteer J, Williams J Jr, Cleveland R, Van Cauwelaert J, Bailey M, Lifshitz D, Evan A. Ultracal-30 gypsum artificial stones for research on the mechanisms of stone breakage in shock wave lithotripsy. Urol Res. 2005; 33(6):429–434. [PubMed: 16133577]

Park SJ, Yi BH, Lee HK, Kim YH, Kim GJ, Kim HC. Evaluation of patients with suspected ureteral calculi using sonography as an initial diagnostic tool: how can we improve diagnostic accuracy? J Ultrasound Med. 2008; 27(10):1441–1450. [PubMed: 18809954]

Rahmouni A, Bargoin R, Herment A, Bargoin N, Vasile N. Color Dopplertwinkling artifact in hyperechoic regions. Radiology. 1996; 199(1):269–271. [PubMed: 8633158]

Rubaltelli L, Khadivi Y, Stramare R, Candiani F, Torraco A, Tregnaghi A. Power Doppler signals produced by static structures: a frequent cause of interpretation errors inthe study of slow flows. Radiol Med. 2000; 99(3):161–164. [PubMed: 10879163]

Shang M, Sun X, Liu Q, Li J, Shi D, Ning S, Cheng L. QuantitativeEvaluation of the Effects of Urinary Stone Composition and Size on Color Doppler Twinkling Artifact: A Phantom Study. J Ultrasound Med. 2017; 36(4):733–740. DOI: 10.7863/ultra.16.01039 [PubMed: 28039937]

Shivaprasad V, Govardhanan Vuyyuru V, Katankot N, Raju V, SUB. Doppler parameters in elicitation of twinkling artefacts in suspected cases of renal calculi. JEBMH. 2016; 3(57):2958–2691.

Sorensen MD, Harper JD, Hsi RS, Shah AR, Dighe MK, Carter SJ, Moshiri M, Paun M, Lu W, Bailey MR. B-mode Ultrasound Versus Color Doppler Twinkling Artifact in Detecting Kidney Stones. J Endourology. 2013; 27(2):149–153. DOI: 10.1089/end.2012.0430

Tanabe M, Naito Y, Nishimoto M, Liu L. Effect of pulse repetition frequency on microcalcification detection in color flow imaging. Jap J Appl Phys. 2014; 53:07KF15.

Turrin A, Minola P, Costa F, Cerati L, Andrulli S, Trinchieri A. Diagnostic value of colour Doppler twinkling artefact in sites negative for stones on B mode renal sonography. Urol Res. 2007; 35(6): 313–317. DOI: 10.1007/s00240-007-0110-8 [PubMed: 17874239]

Williams JC, McAteer JA, Evan AP, Lingeman JE. Micro-computed tomography for analysis of urinary calculi. Urological Res. 2010; 38(6):477–484. DOI: 10.1007/s00240-010-0326-x

Williams JC, Saw KC, Paterson RF, Hatt EK, McAteer JA, Lingeman JE. Variability of renal stone fragility in shock wave lithotripsy. Urology. 2003; 61(6):1092–1096. DOI: 10.1016/S0090-4295(03)00349-2 [PubMed: 12809867]

Winkel RR, Kalhauge A, Fredfeldt KE. The Usefulness of Ultrasound Colour-Doppler Twinkling Artefact for Detecting Urolithiasis Compared with Low Dose Nonenhanced Computerized Tomography. Ultrasound Med Biol. 2012; 38(7):1180–1187. DOI: 10.1016/j.ultrasmedbio.2012.03.003 [PubMed: 22502894]

Worcester EM, Coe FL. Nephrolithiasis. Prim Care. 2008; 35(2):369–91. DOI: 10.1016/j.pop.2008.01.005 [PubMed: 18486720]

Zarse CA, McAteer JA, Sommer AJ, Kim SC, Hatt EK, Lingeman JE, Evan AP, Williams JC. Nondestructive analysis of urinary calculi using micro computed tomography. BMC Urology. 2004; 4(1):15.doi: 10.1186/1471-2490-4-15 [PubMed: 15596006]

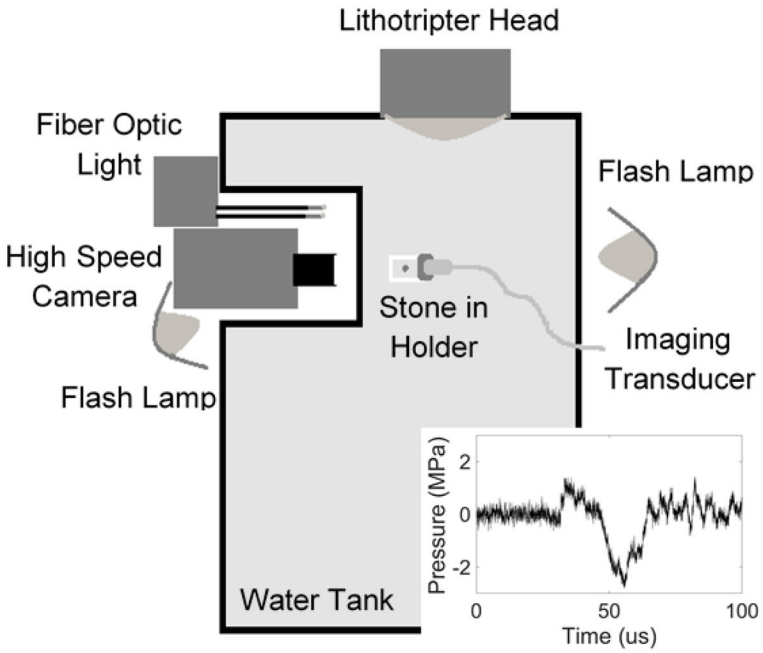


**Figure 1.**

Experimental arrangement to visualize crevice bubbles on the kidney stone surface by expanding them with a lithotripter pulse. Stones were placed pre-focal and off axis and were visualized with a high-speed camera and ultrasound transducer when the lithotripter pulse (inset) arrived.

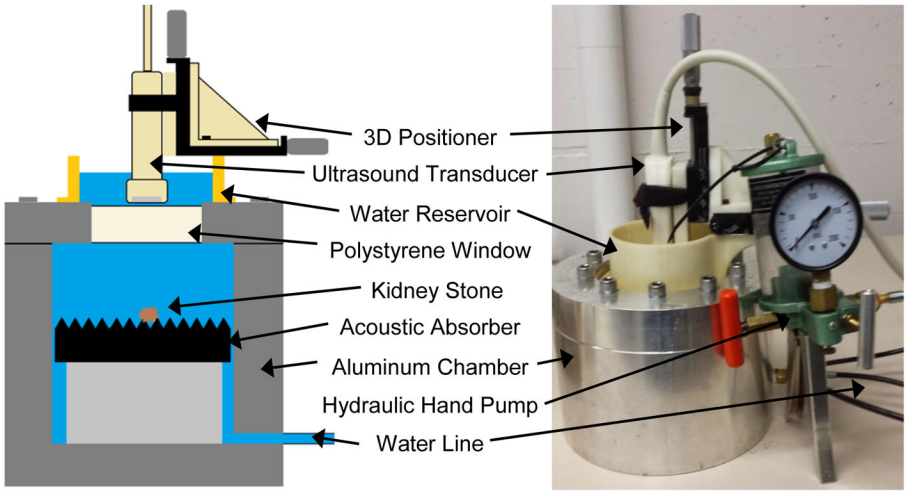


**Figure 2.**

Schematic (left) and photograph (right) of the aluminum-walled hyperbaric chamber. The diagram shows the internal arrangement of the tank for the hyperbaric and hypobaric experiments.

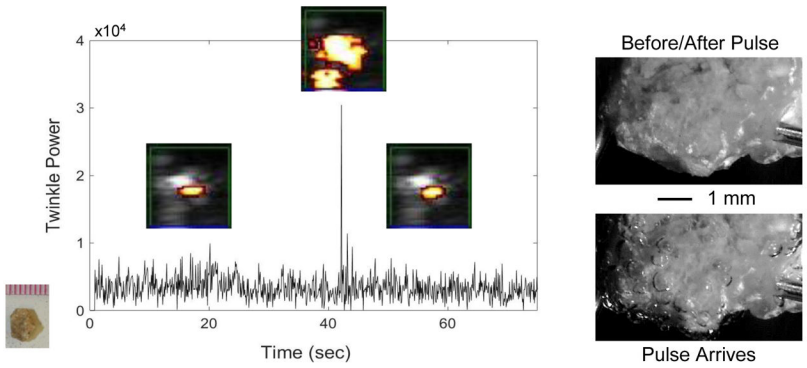


**Figure 3.**

Plot of twinkle power versus time before, during, and after a pre-focal, off axis lithotripter pulse arrives at a COM stone. Overlaid on the plot are selected ROI Doppler images (image scale: 1-cm width) showing the stone (grey) and twinkling (color) on the stone. When the lithotripter pulse arrives at about 45 sec, bubbles are excited on the stone surface, as observed with high-magnification, high-speed photography *(right)*, and twinkle power increases transiently (for one Doppler imaging frame) by more than six times. After the lithotripter pulse and cessation of bubble oscillation, twinkling returns to approximately initial levels. These data were collected with the P4-2 transducer.

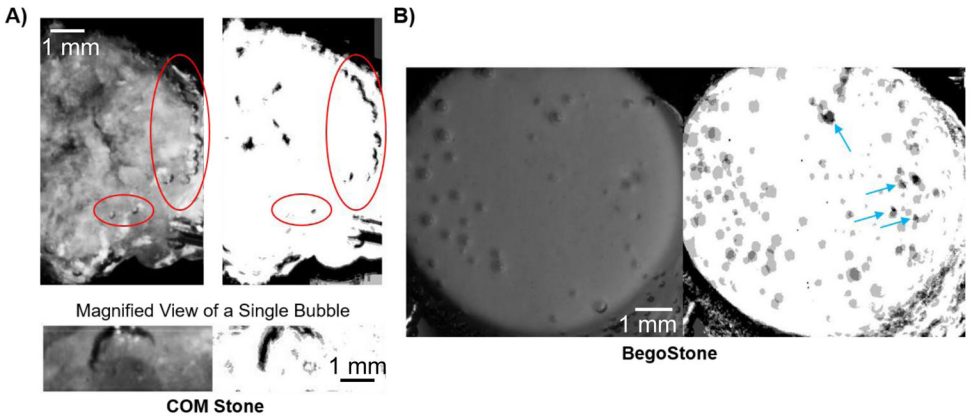


**Figure 4.**

Each set of images shows *(left)* a high-speed photograph of bubbles on the stone surface from a single lithotripter pulse and *(right)* the average of four binary images from repeated lithotripter pulses for A) a COM stone and B) a BegoStone. In A), a chain of bubbles arose on the right side of the stone with every pulse, as indicated by the black bubble outline in the binary image. While not every bubble arose with each lithotripter pulse, bubbles repeatedly arose from certain locations on the stone surface. The magnified image shows the dark outline of a bubble that arose in one particular location in all four lithotripter pulses. In B), the bubble distribution was variable with successive lithotripter pulses, as evidenced by the grey as opposed to black scattered across the stone surface in the binary image. Blue arrows indicate the four locations on the BegoStone surface with noticeable imperfections that could not be filtered out of the binary image.

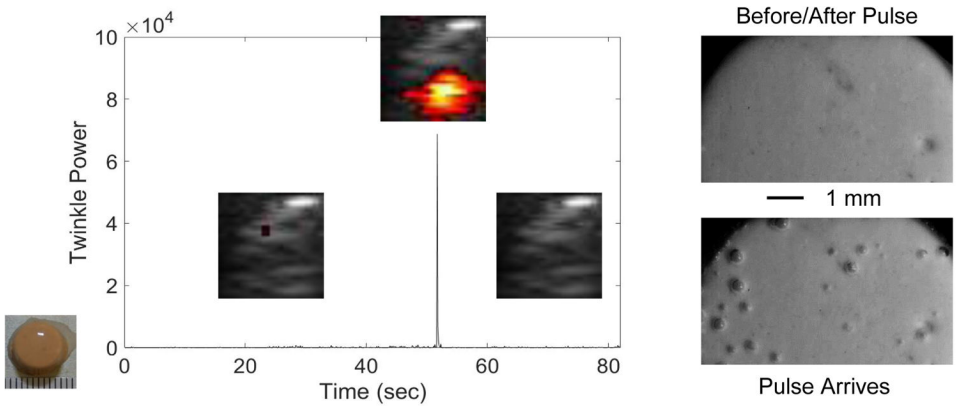


**Figure 5.**

Plot of twinkle power versus time before, during, and after a pre-focal, off axis lithotripter pulse arrives at a cylindrical, artificial BegoStone. Overlaid on the plot are selected ROI Doppler images (image scale: 1-cm width) showing the stone (grey) and twinkling in color (if present). Twinkling is virtually nonexistent until the lithotripter pulse arrived at about 52 sec. When the pulse arrives, bubbles are excited on the BegoStone surface as observed with high-magnification, high-speed photography *(right),* and twinkling increases significantly for the duration of the pulse plus time for bubble oscillations. After the lithotripter pulse, twinkling returned to initial levels of little to no twinkling. These data were collected with the P4-2 transducer.

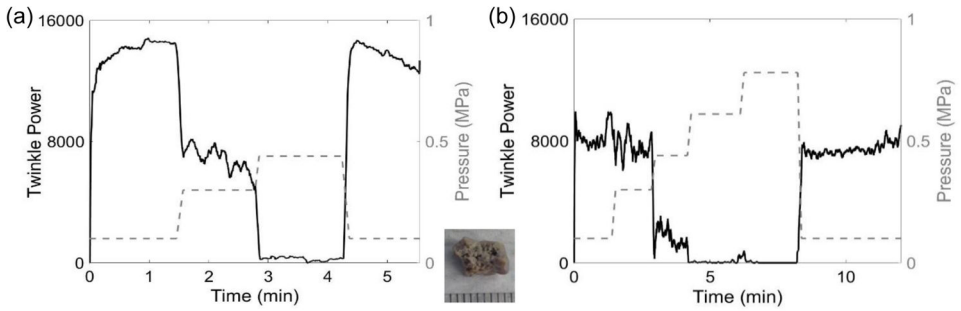


**Figure 6.**

Plots of twinkle power versus time and absolute static pressure in MPa (dashed grey line, right axis) showing the response of the same COM stone (shown in inset) to hyperbaric pressures with (a) taken 24 hours before (b). Both plots show similar trends; however, the hyperbaric threshold to eliminate twinkling is >2 times higher in (b) compared to (a). These data were collected with the L7-4 transducer.

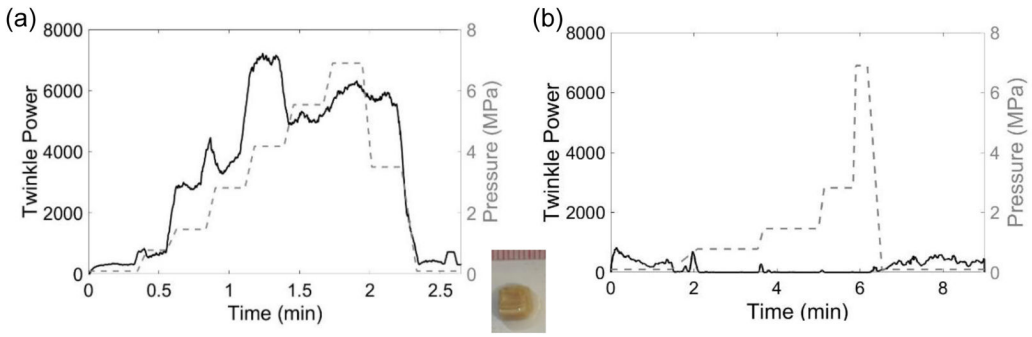


**Figure 7.**

Plots of twinkle power versus time and absolute static pressure in MPa (dashed grey line, right axis) showing the effect of hyperbaric pressures for the same brushite stone (shown in inset) with the plot in (a) taken 4 days before the plot in (b). Twinkling is found to increase with hyperbaric pressures in (a), whereas twinkling decreases with the increasing pressure in (b). In both cases, twinkle powers are similar at both the beginning and the ends of the plots. These data were collected with the P4-2 transducer.

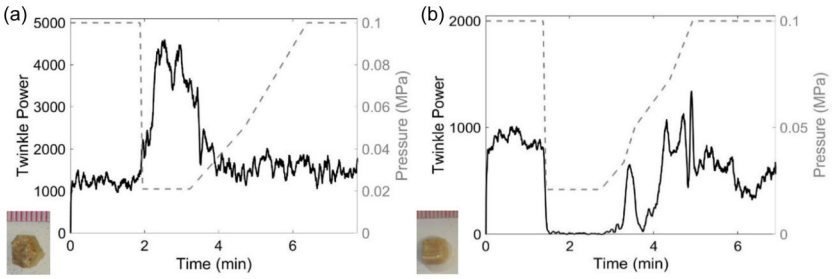


**Figure 8.**

Plots of twinkle power versus time and absolute static pressure in MPa (dashed, right y-axis) showing the effect of hypobaric conditions on (a) COM and (b) brushite stones. (a) When pressure was reduced, the twinkle power on the macroscopically rough COM stone increased before returning to initial levels when the pressure was returned to atmosphere. (b) Twinkling on the macroscopically smooth brushite stone decreased when the pressure was reduced before returning to approximately the initial levels when the pressure was returned to atmosphere. These data were collected with the P4-2 transducer.

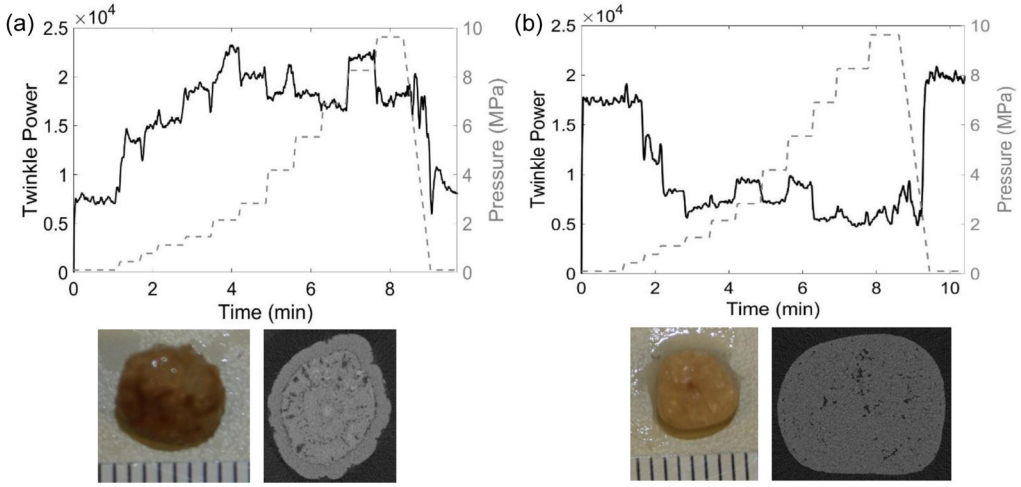


**Figure 9.**

Plots of twinkle power versus time and absolute static pressure (MPa; right y-axis) for (a) a calcium oxalate dihydrate (COD) stone and (b) a cystine stone. (a) The μCT cross section of this COD stone shows a slightly rough stone surface with a ringed structure and some internal micro-crevices comprising 8.6% of the center slice area. The twinkle power was initially of moderate amplitude and generally increased with pressure. (b) The μCT cross section of this cystine stone shows a macroscopically smooth surface with a scattering of micro-crevices throughout the stone comprising 3.7% of the center slice void. Twinkling was initially quite strong and decreased with elevated pressure and then stayed at a constant, non-zero level. In both cases, twinkling returned to its initial amplitude when pressure was returned to ambient levels. These data were collected with the P4-2 transducer.

**Table 1**

Number and primary composition of stones used.

| Stone Composition | Number Evaluated |
|---|---|
| Calcium Oxalate Monohydrate (COM) | 8 |
| Uric Acid | 6 |
| Calcium Oxalate Dihydrate (COD) | 5 |
| Cystine | 5 |
| Brushite | 3 |
| Begostone and U30 Artificial Stones | 6 |